

Scalable Heterogeneous Graph Learning via Heterogeneous-aware Orthogonal Prototype Experts

Wei Zhou¹ Hong Huang¹ Ruize Shi¹ Bang Liu²

Abstract

Heterogeneous Graph Neural Networks (HGNNs) have advanced mainly through better encoders, yet their decoding/projection stage still relies on a single shared linear head, assuming it can map rich node embeddings to labels. We call this the Linear Projection Bottleneck: in heterogeneous graphs, contextual diversity and long-tail shifts make a global head miss fine semantics, overfit hub nodes, and underserve tail nodes. While *Mixture-of-Experts* (MoE) could help, naively applying it clashes with structural imbalance and risks expert collapse. We propose a **Heterogeneous-aware Orthogonal Prototype Experts** framework named **HOPE**, a plug-and-play replacement for the standard prediction head. HOPE uses learnable prototype-based routing to assign instances to experts by similarity, letting expert usage follow the natural long-tail distribution, and adds expert orthogonalization to encourage diversity and prevent collapse. Experiments on four real datasets show consistent gains across SOTA HGNN backbones with minimal overhead.

1. Introduction

Heterogeneous Graphs (HG) serve as a powerful abstraction for modeling complex systems containing multiple types of nodes and edges. The proliferation of *Heterogeneous Graph Neural Networks* (HGNNs) has significantly advanced the state-of-the-art in tasks such as node classification and link prediction (Zhou et al., 2023; 2024). Pioneering architectures like R-GCN (Schlichtkrull et al., 2018), HGT (Hu et al., 2020), and the recent scalable Se-

¹National Engineering Research Center for Big Data Technology and System, Services Computing Technology and System Lab, Cluster and Grid Computing Lab, School of Computer Science and Technology, Huazhong University of Science and Technology, Wuhan, 430074, China. ²DIRO, Université de Montréal & Mila & Canada CIFAR AI Chair, Canada. Correspondence to: Hong Huang <honghuang@hust.edu.cn>.

HGNN (Yang et al., 2023) and HGMLP (Liang et al., 2024b) have focused predominantly on the encoding phase, designing intricate mechanisms to aggregate heterogeneous neighbors and fuse multi-modal semantics into a unified node representation.

However, a critical yet overlooked limitation persists in the decoding or projection phase of these frameworks. The prevailing paradigm implicitly assumes that a single, global linear transformation (followed by Softmax) has sufficient capacity to map the learned high-dimensional representations onto the label space. We identify this assumption as the “**Fixed Linear Projection Bottleneck**” in HG representation learning.

This bottleneck is particularly severe in HGs due to two intrinsic characteristics. **1. Contextual Diversity.** A node’s semantic meaning is always context-dependent (Dong et al., 2017; Wang et al., 2019). For instance, in an academic graph, an author node might behave as a “theoretician” in one collaboration subgraph but as an “applied scientist” in another. A static, global projection head forces the encoder to compress these multifaceted roles into a single vector that satisfies an average linear decision boundary, inevitably losing fine-grained semantic nuances. **2. Long-tail Distribution Shift.** Real-world graphs follow long-tail distributions (Wang et al., 2020; Yang et al., 2022). High-degree “hub” nodes dominate the gradient updates, causing the global projection matrix to overfit to majority patterns. Consequently, “tail” nodes, which often require specialized decision boundaries due to their sparse connectivity (Liu et al., 2021; Liang et al., 2024a), are poorly served by this global shared head.

Mixture-of-Experts (MoE) presents a promising avenue to break this bottleneck. By conditionally activating specialized parameters for different inputs, MoE theoretically allows the model to master diverse semantic patterns without exploding computational costs (Cai et al., 2025; Mu & Lin, 2025). However, directly transplanting standard MoE architectures to HGs is non-trivial and fraught with domain-specific challenges. **1. Structural Imbalance vs. Load Balancing.** Standard MoE frameworks typically enforce strict load balancing to ensure all experts are utilized equally (Zeng et al., 2025). However, HGs inherently ex-

hibit severe long-tail distributions in node types and relation frequencies (Wang et al., 2020; Yang et al., 2022). A “hub” node appears exponentially more often than a “tail” type. Forcing a uniform load distribution across experts contradicts this natural data skewness, potentially coercing experts to process node types they are ill-equipped for, thereby degrading performance on both hub and tail classes. **2. Expert Collapse.** Without explicit routing regularization (e.g., load-balancing), MoE models may suffer from routing degeneracy and insufficient expert specialization, leading to redundant experts and reduced benefits of conditional computation (Li et al., 2024; Qiu et al., 2025). In graph settings with heterogeneous and long-tailed semantics, this risk can be exacerbated, motivating additional diversity or balance constraints.

To address these fundamental limitations, we propose a **Heterogeneous-aware Orthogonal Prototype Experts** framework named **HOPE**. HOPE is explicitly designed to adapt to the heterogeneous information and long-tail semantic distributions inherent in graph-structured data, thereby enhancing the model’s capacity to capture fine-grained, instance-specific patterns. HOPE introduces a learnable, prototype-based routing mechanism that assigns nodes to experts based on embedding similarity. This approach resolves the conflict between enforced load balancing and the graph’s intrinsic long-tail distribution, allowing experts to specialize in distinct semantic regions, including rare patterns. Furthermore, we incorporate a tailored orthogonalization strategy that enforces orthogonality among dynamic experts. This maximizes semantic diversity and prevents expert collapse, ensuring complementary expertise for complex semantics. Functioning as a universal plug-and-play module, HOPE can replace the standard prediction head in various HGNN backbones. Extensive experiments on four real-world datasets demonstrate that HOPE consistently enhances the performance of state-of-the-art architectures with minimal computational overhead.

Our contributions can be summarized as follows:

- **Universal Projection Paradigm.** We identify the fixed linear head as a bottleneck for polysemous and long-tail nodes. HOPE introduces a model-agnostic hybrid expert layer, serving as a universal plugin to enhance diverse HGNN encoders.
- **Orthogonal Experts & Prototype Routing.** We propose expert orthogonalization to maximize functional diversity and prevent mode collapse, coupled with a prototype-based routing mechanism that mitigates load imbalance by assigning nodes via semantic similarity.
- **SOTA Performance & Compatibility:** Extensive experiments on four datasets confirm that HOPE consistently boosts multiple SOTA backbones with negligible overhead, proving its value as a practical, general-purpose enhancement.

2. Methodology

In this section, we first formulate the problem and the limitations of standard projections. We then detail the HOPE architecture, focusing on the prototype routing mechanism and orthogonal constraint. Finally, we provide a theoretical analysis of the routing properties and a comprehensive complexity analysis.

2.1. Preliminaries and Motivation

Let $\mathcal{G} = (\mathcal{V}, \mathcal{E})$ denote a heterogeneous graph. We assume a backbone encoder \mathcal{F} maps each node v to a set of semantic-specific embeddings $\mathcal{H}_v = \{\mathbf{h}_v^{\Phi_1}, \dots, \mathbf{h}_v^{\Phi_M}\}$, where $\mathbf{h}_v^{\Phi_m} \in \mathbb{R}^d$ corresponds to the m -th meta-path view.

The Fixed Linear Projection Bottleneck. We define the bottleneck as a compound limitation inherent in standard HGNN decoders, arising from the mismatch between rigid model architectures and the dynamic nature of heterogeneous data. It manifests in two aspects:

- **Fixed Capacity Constraint.** Existing heads enforce a uniform computational budget (e.g., a fixed k -expert routing or dense aggregation) across all nodes. This ignores the long-tail distribution of node semantics, causing information loss for semantic-rich “hub” nodes (under-fitting) and introducing noise for sparse “tail” nodes (over-smoothing).
- **Linear Separability Assumption.** The reliance on a global linear projection implicitly assumes that complex node embeddings are linearly separable. This fails to capture the severe contextual polysemy and distribution shifts, limiting the model’s ability to resolve non-linear decision boundaries in the latent space.

2.2. Overview of HOPE Framework

To overcome the limitations of linear projections, we propose **HOPE** (Heterogeneous-aware Orthogonal Prototype Experts). As shown in Figure 1, HOPE is a plug-and-play neural projection framework that transforms the traditional decoding layer into a MoE system. It accepts representations from any HGNN backbone and refines them to handle inherent long-tail distributions. Instead of strict load balancing, HOPE employs a **prototype routing mechanism**, selecting experts based on semantic similarity to learnable prototypes to naturally adapt to data skewness. Furthermore, an **elastic capacity mechanism** dynamically adjusts the number of active experts based on feature quality under a global budget. Architecturally, the projection is decoupled

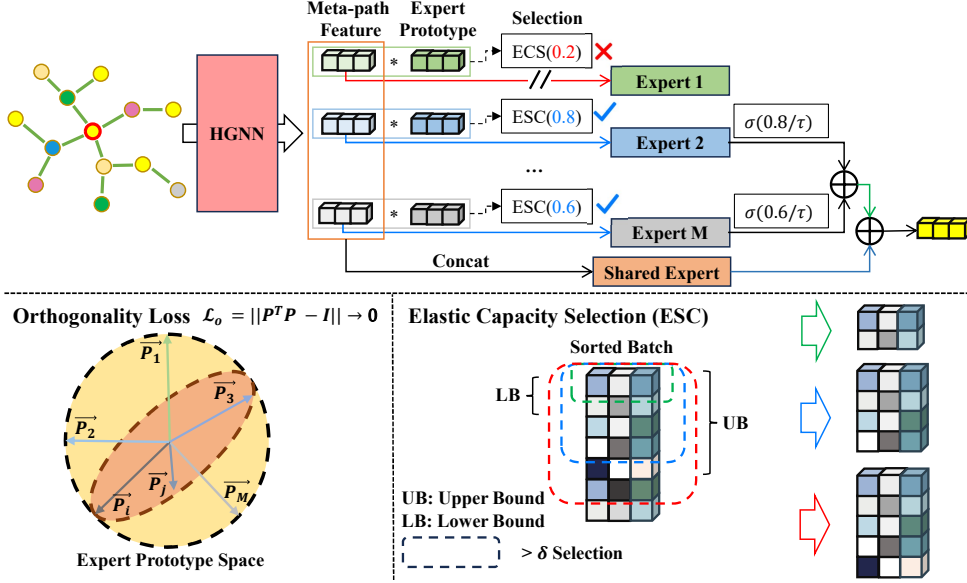


Figure 1. The structure of HOPE.

into two independent pathways: 1. Shared Pathway. Captures stable, universal structural patterns across the graph. 2. Dynamic Pathway. Sparsely activated to handle instance-specific semantic nuances. To prevent redundancy and mode collapse, we enforce strict orthogonality among dynamic experts. By replacing standard prediction heads, HOPE effectively unlocks the backbone’s potential in modeling complex heterogeneity with minimal computational overhead.

2.3. Input and Context Encoding

Given a heterogeneous graph $\mathcal{G} = (\mathcal{V}, \mathcal{E})$ and a set of pre-defined meta-paths $\mathcal{M} = \{\Phi_1, \Phi_2, \dots, \Phi_M\}$, we assume a backbone encoder \mathcal{F}_θ produces a set of semantic-specific embeddings for each node v

$$\mathcal{H}_v = \{\mathbf{h}_v^{\Phi_1}, \mathbf{h}_v^{\Phi_2}, \dots, \mathbf{h}_v^{\Phi_M}\}, \quad (1)$$

where $\mathbf{h}_v^{\Phi_m} \in \mathbb{R}^d$ captures the node semantics under the m -th meta-path view. To provide a holistic view for the global stability analysis, we also construct a concatenated representation

$$\mathbf{h}_v^{\text{all}} = \text{Concat}(\mathbf{h}_v^{\Phi_1}, \dots, \mathbf{h}_v^{\Phi_M}) \in \mathbb{R}^{M \cdot d}. \quad (2)$$

2.4. Hybrid Expert Mechanism

HOPE employs a hybrid architecture where experts are explicitly aligned with meta-path views to balance global structural stability and local semantic selection.

2.4.1. SHARED PATHWAY

To capture cross-view dependencies and universal patterns by observing the complete semantic context simultaneously. We deploy a shared expert S . The input to this pathway is the concatenated feature vector $\mathbf{h}_v^{\text{all}}$. The stability representation $\mathbf{z}_v^{(s)}$ is computed as

$$\mathbf{z}_v^{(s)} = S(\mathbf{h}_v^{\text{all}}), \quad (3)$$

where S is a *Multilayer Perceptron* (MLP). By processing the full spectrum of meta-paths, the shared expert ensure that the model retains a comprehensive understanding of the node’s global context.

2.4.2. DYNAMIC PATHWAY

To adaptively select and refine the most discriminative meta-path views for each specific node instance. Distinct from generic MoEs, we design the dynamic expert bank to strictly correspond to the meta-path set. We instantiate M dynamic experts $\{D_1, \dots, D_M\}$, where the m -th expert D_m is dedicated to processing the specific feature $\mathbf{h}_v^{\Phi_m}$.

Semantic-Aware Gating. Each expert D_m is associated with a learnable prototype $\mathbf{p}_m \in \mathbb{R}^d$, representing the ideal semantic signature for that meta-path view. Instead of a global routing competition, the activation of expert m is determined by the alignment between its specific input $\mathbf{h}_v^{\Phi_m}$ and its prototype \mathbf{p}_m . The relevance score is

$$s_{v,m} = \frac{(\mathbf{h}_v^{\Phi_m})^\top \mathbf{p}_m}{\|\mathbf{h}_v^{\Phi_m}\|_2 \|\mathbf{p}_m\|_2}. \quad (4)$$

Elastic Capacity Selection. To balance elastic computational resource allocation while preventing expert collapse, we propose a hybrid expert selection mechanism. This mechanism addresses the conflict between signal noise interference and tail node loss in traditional routing strategies through three distinct levels of constraints:

- **Quality Criterion (\mathcal{C}_{Qual}) — Noise Rejection.** To ensure experts only process high-confidence samples and avoid interference from irrelevant signals during feature learning, we set a hard threshold δ , considering only nodes with semantic alignment $s_{v,m} > \delta$. This constitutes the primary filtering barrier.
- **Stability Criterion (\mathcal{C}_{Stab}) — Tail Preservation.** Targeting “long-tail” nodes with weak feature representations that are easily filtered out by thresholds (i.e., hard samples), the expert enforces the inclusion of the Top- K best-matching nodes in the batch (as a lower bound) to prevent them from becoming unassigned “orphan nodes” and causing information loss. This provides a survival guarantee mechanism.
- **Capacity Criterion (\mathcal{C}_{Cap}) — Load Control.** Constrained by the computational budget, to prevent specific experts from overloading and to maintain system efficiency, we ultimately retain only the highest-scoring Top- C nodes (as an upper bound) from the union of the above two criteria. This achieves memory-friendly elastic truncation.

Formally, the selection mask $M_{v,m} \in \{0, 1\}$ is defined as

$$M_{v,m} = \begin{cases} 1 & \text{if } v \in \text{Top-}C(\Omega_m) \\ 0 & \text{otherwise} \end{cases}, \quad (5)$$

where $\Omega_m = \mathcal{S}_{Qual}^{(m)} \cup \mathcal{S}_{Stab}^{(m)}$ denotes the candidate pool, $\mathcal{S}_{Qual}^{(m)} = \{u \mid s_{u,m} > \delta\}$ represents the high-confidence node set filtered by semantic alignment, and $\mathcal{S}_{Stab}^{(m)} = \text{Top-}K(\mathbf{s}_{:,m})$ is the mandatory set of the top- K best-matching nodes serving as a stability guarantee.

Gated Aggregation. For the selected node-expert pairs, we compute a gating weight using a Sigmoid function with temperature τ as

$$g_{v,m} = \sigma(s_{v,m}/\tau) \cdot M_{v,m}, \quad (6)$$

where τ is a trainable parameter. The dynamic representation $\mathbf{z}_v^{(d)}$ is the sparse weighted sum of activated experts

$$\mathbf{z}_v^{(d)} = \sum_{m=1}^M g_{v,m} \cdot D_m(\text{LayerNorm}(\mathbf{h}_v^{\Phi_m})). \quad (7)$$

2.4.3. ADAPTIVE FUSION

The final node representation \mathbf{z}_v fuses the global context from the shared pathway and the selected semantics from the dynamic pathway via a projection matrix $\mathbf{W}_{\text{fusion}}$ as

$$\mathbf{z}_v = \mathbf{W}_{\text{fusion}} [\mathbf{z}_v^{(s)} \parallel \mathbf{z}_v^{(d)}] + \mathbf{b}. \quad (8)$$

2.5. Orthogonality Constraint

To ensure that different meta-path experts represent distinct semantic directions. Even though experts are tied to different meta-paths, their prototypes should remain distinct to prevent semantic overlap. We enforce orthogonality on the prototype matrix $\mathbf{P} = [\mathbf{p}_1, \dots, \mathbf{p}_M]$ as

$$\mathcal{L}_{\text{o}} = \|\mathbf{P}^\top \mathbf{P} - \mathbf{I}\|_F^2 = \sum_{i \neq j} \left(\frac{\mathbf{p}_i^\top \mathbf{p}_j}{\|\mathbf{p}_i\|_2 \|\mathbf{p}_j\|_2} \right)^2. \quad (9)$$

The total objective function is:

$$\mathcal{L} = \mathcal{L}_t + \lambda \mathcal{L}_{\text{ortho}}, \quad (10)$$

where \mathcal{L}_t denotes the target loss of downstream tasks.

2.6. Theoretical Analysis

We analyze the effectiveness of the proposed Elastic Capacity Selection mechanism from the perspectives of gradient flow preservation and noise robustness.

Robustness against Representation Collapse. Consider a scenario where a specific meta-path view Φ_{noise} generates non-informative features for a subset of nodes \mathcal{V}_{sub} , resulting in alignment scores $s_{v,\Phi_{noise}} \approx 0, \forall v \in \mathcal{V}_{sub}$. In standard Top- k routing (where k is fixed), if other experts are saturated, the noisy expert D_{noise} is forced to process k nodes, introducing variance σ_{noise}^2 into the optimization landscape. In HOPE, the Quality Criterion (\mathcal{C}_{Qual}) with threshold δ ensures that if $\max_{v \in \mathcal{B}} s_{v,\Phi_{noise}} < \delta$, the active set size approaches the lower bound $|\Omega_{noise}| \rightarrow K$. Since $K \ll C$ (typically $K = 1$), the injection of noise is strictly bounded, minimizing the interference term in the gradient update $\nabla_{\theta} \mathcal{L}$.

Gradient Preservation for Tail Nodes. Let v_{tail} be a hard sample with weak semantic features such that its maximum alignment score $\max_m s_{v_{tail},m} < \delta$. Under a pure thresholding strategy (e.g., vanilla sparse gating), the gating weights would be zeroed out ($g_{v_{tail},m} = 0, \forall m$), leading to the “dead node” problem where $\frac{\partial \mathcal{L}}{\partial \mathbf{h}_{v_{tail}}} \rightarrow \mathbf{0}$. The Stability Criterion (\mathcal{C}_{Stab}) guarantees that v_{tail} is included in the candidate set Ω_{m^*} of its relatively best-matching expert $m^* = \arg \max_m s_{v_{tail},m}$. This ensures a non-zero gradient flow path back to the backbone encoder, preventing the feature learning stagnation often observed in long-tail distributions.

Semantic Disentanglement. The orthogonality constraint on prototypes \mathcal{L}_o minimizes the cosine similarity between expert directions. This effectively pushes the expert prototypes p_m to span the maximal volume in the feature space \mathbb{R}^d . Consequently, the Semantic-Aware Gating becomes a projection onto a nearly orthogonal basis, maximizing the discriminative power of the routing mechanism compared to random initialization or dense attention mechanisms.

2.7. Complexity Analysis

We demonstrate that HOPE achieves superior representational capacity with a computational cost comparable to standard GNNs, maintaining linear scalability with respect to batch size.

Time Complexity. Let $|\mathcal{B}|$ be the batch size, d the hidden dimension, M the number of meta-paths, and L the number of layers in each MLP expert.

- **Backbone & Pre-processing:** Generating meta-path embeddings takes similar time to exist HGNN models.
- **Shared Pathway:** The shared expert S processes the concatenated input for all nodes. Since the input dimension is $M \cdot d$, the first layer costs $O(|\mathcal{B}| \cdot (M \cdot d) \cdot d)$, and subsequent $L - 1$ layers cost $O(|\mathcal{B}| \cdot d^2)$. Thus, the total cost is $O(|\mathcal{B}| \cdot d^2 \cdot (M + L))$.
- **Routing Decision:** Computing alignment scores $s_{v,m}$ requires dot products between node features and prototypes: $O(|\mathcal{B}| \cdot M \cdot d)$. The selection process (Top- K and filtering) is efficient on GPUs, typically dominated by the score computation.
- **Dynamic Execution (Sparse):** Crucially, experts in the dynamic pathway only process a subset of nodes. Let ρ be the average sparsity ratio (active nodes / total nodes) determined by the Elastic Capacity Selection ($\rho \ll 1$). Each dynamic expert is an L -layer MLP. The computation cost is $O(\rho \cdot |\mathcal{B}| \cdot M \cdot L \cdot d^2)$.

The overall time complexity is roughly $O(|\mathcal{B}| \cdot d^2 \cdot (M + \rho M L))$. Since $\rho M \approx \text{const}$ (average active experts per node) and L is small, HOPE is asymptotically linear with respect to $|\mathcal{B}|$.

Space Complexity. The parameter overhead is minimal compared to the performance gain:

- **Model Parameters:** We store M dynamic experts and 1 shared expert. Assuming each expert has L layers of width d , the parameters are approximately $O((M + 1) \cdot L \cdot d^2)$. Since M is typically small (e.g., $M < 10$) in HG datasets, this is negligible compared to large-scale graph adjacency matrices.

Table 1. Dataset statistics.

Dataset	#Node	#Edge	Task
Freebase	180,098	2,115,376	NC
Ogbn-mag	1,939,743	42,222,014	NC
DBLP	1,989,077	376,486,176	NC/LP
Yelp	8,2465	30,542,675	LP

- **Routing Prototypes:** Storing M prototype vectors requires only $O(M \cdot d)$.
- **Memory Usage:** The gating mechanism utilizes a sparse selection mask, avoiding the storage of a dense $|\mathcal{B}| \times M$ intermediate activation tensor, making HOPE memory-efficient for large batches.

3. Experiments

In this section, we rigorously evaluate HOPE on several real-world datasets. We aim to answer the following questions:

- **RQ1 (Performance & Efficiency):** Can the proposed HOPE architecture help HGNN models perform better with acceptable additional overhead?
- **RQ2 (Ablation Study):** Are the shared pathway, Orthogonality constraints, and elastic capacity selection necessary for performance?
- **RQ3 (Parameter Sensitivity):** How do the similarity threshold δ , lower bound K , upper bound C , and orthogonality constraint weight λ affect model behavior?

3.1. Experimental Setup

Datasets. To demonstrate the performance and efficiency of HOPE, a general-purpose performance enhancement strategy, we evaluate it on two types of tasks: node classification and link prediction. The node classification task includes three heterogeneous graphs (Freebase (Lv et al., 2021a), Ogbn-mag (Wang et al., 2020), and DBLP (Yang et al., 2022)). The link prediction task includes two heterogeneous graphs (Yelp (Yang et al., 2022) and DBLP). Detailed information about the data is presented in Table 1.

Baselines. To evaluate the effectiveness of HOPE, we conduct a comparative analysis of HOPE against existing enhancement techniques. This comparison occurs on two categories of backbone models: 1) traditional methods, such as R-GCN (Schlichtkrull et al., 2018), R-GAT (Veličković et al., 2018), and R-GSN (Wu et al., 2021). 2) state-of-the-art methods that employ specific enhancement techniques, including NARS (Yu et al., 2020), SeHGNN (Yang et al., 2023), and HGMLP (Liang et al., 2024b).

Experimental Settings. All models are trained on the server equipped with the Intel Xeon CPU E5-2680, the Nvidia RTX 5090 (32GB) GPU, and 50GB of memory. The software used was Ubuntu 22.04 and CUDA 11.8. All models are implemented in PyTorch with DGL backend. We use Adam optimizer with learning rate 0.001 and weight decay 0.0. All models are trained for 300 epochs.

For R-GCN, R-GAT, and R-GSN, the hidden dimension is set to 256, with 2-layer architectures. The representation of each hop is passed through an *mlp*, and the average of all layers is then used as the final node representation. When enhanced with HOPE, the input also consists of the representations from each hop. The similarity threshold δ is set to 0.2, lower bound K to 0.5, upper bound C to 3, and the orthogonality constraint weight λ to 0.5. Due to the excessive time complexity of these methods, we use neighbor sampling to reduce time overhead. For all datasets, the number of sampled neighbors is 15 for the first hop and 20 for the second hop.

For NARS, SeHGNN, and HGAMLP, the hidden dimension is set to 512, with 2-layer architectures. When enhanced with HOPE, the input for NARS is the node representations of each heterogeneous subgraph, while the inputs for SeHGNN and HGAMLP are the representations corresponding to each meta-path. The similarity threshold δ is set to 0.6, lower bound K to 0.5, upper bound C to 3, and the orthogonality constraint weight λ to 0.5.

Except for Ogbn-mag, the node representations for all datasets are generated by ComplEx (Trouillon et al., 2016), whereas in Ogbn-mag, the representations for nodes other than papers are generated by LINE (Tang et al., 2015). The other parameters not mentioned are set to their default values. To obtain accurate results, we repeat all experiment 10 times and take the average (random seeds are [1, 2, 3, 4, 5, 6, 7, 8, 9, 10]).

3.2. Node Classification

To comprehensively evaluate the generality and core advantages of the HOPE architecture, we conduct extensive node classification experiments on three real-world datasets covering varying scales and topological characteristics. The experimental results are shown in Table 2. The experimental results not only fully validate the effectiveness of HOPE in handling diverse data but also reveal the exceptional balance achieved between computational efficiency and model performance. Notably, HOPE significantly enhances the overall classification performance of base models while introducing negligible additional computational overhead, and even demonstrating higher inference efficiency in certain optimized scenarios.

Specifically, in the most challenging experimental settings,

HOPE achieves a performance leap compared to baseline models. This significant quantitative metric strongly confirms that the architecture possesses exceptional robustness and superior scalability when facing complex real-world application scenarios.

Further in-depth analysis indicates that the key to HOPE’s success lies in its fundamental overcoming of the “linear constraint bottleneck” prevalent in traditional methods. Traditional models are often limited by shallow linear expressive capabilities, making it difficult to capture deep interaction features within the data. In contrast, by introducing more expressive non-linear mechanisms, HOPE successfully achieves effective modeling and precise capturing of the implicit, complex non-linear semantic information within the data. This capability enables the model to maintain stable and substantial gains regardless of drastic changes in data scale or severe distribution shifts.

3.3. Ablation Studies

To validate the necessity of each component in the HOPE architecture, we conduct a comprehensive ablation study on the Ogbn-mag dataset using HGAMLP as the backbone model. The relevant results are summarized in Table 3.

Impact of Shared Pathway. Removing the shared pathway results in a significant performance drop. This result strongly confirms the critical role of the shared expert as an “anchor”. By providing a stable global context representation, it effectively mitigates uncertainty in the routing process, enabling dynamic experts to focus on capturing specific local patterns without the extra burden of maintaining global structural information.

Impact of Prototype Experts. In this setting, we remove the expert prototypes and instead use an *mlp* to assign nodes to experts. Each node selects the top-2 experts. Additionally, we incorporate a load balancing loss with a weight of 0.5 to ensure that no experts are starved. The results show that replacing prototype-based routing with a standard *mlp* router leads to a noticeable drop in performance. This suggests that the semantic guidance provided by the prototypes is crucial for accurate expert assignment. The *mlp* router, despite the load balancing loss, struggles to effectively cluster semantically similar nodes to the appropriate experts, resulting in suboptimal feature specialization and reduced overall classification accuracy.

Impact of Elastic Capacity. In this setting, we remove the lower and upper bounds on expert capacity. We observe that this setting leads to the most significant performance degradation, highlighting the importance of the “leave no node behind” principle. For nodes with weak features or those in the long-tail distribution, forcibly assigning experts (even with slightly lower matching scores) ensures effective

Table 2. Node classification results. OOM denotes Out of Memory, and table shows the time spent in one epoch.

	Freebase				Ogbn-mag				DBLP			
	#Parma	Training	Inferring	Accuracy	#Parma	Training	Inferring	Accuracy	#Parma	Training	Inferring	Accuracy
R-GCN	0.12M	0.22s	6.83s	61.19 ± 0.22	0.19M	103.62s	18.22s	35.34 ± 0.61	0.13M	4.67s	6.79s	42.17 ± 2.47
w. HOPE	0.15M	0.17s	6.90s	63.02 ± 0.14	0.21M	108.11s	20.03s	38.43 ± 0.52	0.16M	5.24s	5.83s	53.56 ± 0.49
R-GAT	0.12M	0.25s	7.34s	62.06 ± 0.25	0.19M	132.81s	21.83s	34.28 ± 0.17	0.13M	4.46s	6.39s	43.30 ± 0.49
w. HOPE	0.15M	0.24s	7.32s	63.97 ± 0.23	0.24M	109.64s	21.36s	38.97 ± 0.37	0.16M	5.47s	5.88s	55.27 ± 2.47
R-GSN	0.17M	0.35s	8.60s	63.98 ± 1.02		OOM			0.18M	4.84s	6.65s	53.28 ± 2.47
w. HOPE	0.18M	0.36s	8.54s	65.55 ± 0.82		OOM			0.19M	5.62s	6.54s	58.12 ± 2.26
NARS	4.0M	0.04s	0.65s	66.97 ± 0.17	4.1M	8.12s	11.11s	52.49 ± 0.22	4.1M	0.01s	28.67s	54.99 ± 0.99
w. HOPE	4.3M	0.05s	0.69s	68.33 ± 0.19	4.6M	9.01s	12.74s	56.87 ± 0.35	4.6M	0.02s	30.19s	57.03 ± 0.83
SeHGNN	56.5M	0.12s	0.62s	64.88 ± 0.16	9.26M	7.57s	0.46s	57.76 ± 0.13	10.1M	0.02s	15.62s	50.14 ± 1.45
w. HOPE	75.9M	0.15s	0.63s	66.73 ± 0.52	11.9M	8.21s	0.46s	57.95 ± 0.14	13.6M	0.02s	15.96s	51.28 ± 0.69
HGAMLP	56.1M	0.18s	0.53s	65.67 ± 0.57	8.86M	5.78s	0.45s	57.89 ± 0.12	9.66M	0.02s	11.16s	49.86 ± 1.07
w. HOPE	75.6M	0.20s	0.56s	67.90 ± 0.13	11.5M	6.76s	0.43s	58.01 ± 0.12	13.3M	0.02s	11.04s	50.47 ± 0.40

Table 3. Ablation Study on Ogbn-mag with backbone HGAMLP.

Variant	Train	Infer	Acc
HOPE (Full Model)	6.76s	0.43s	58.01
w/o Shared Pathway	6.24s	0.30s	57.13
w/o Prototype Experts	5.98s	0.28s	55.36
w/o Elastic Capacity	6.04s	0.35s	57.44
w/o \mathcal{L}_o	6.63s	0.41s	57.38

gradient backpropagation. This prevents them from becoming “dead nodes” that cannot be updated, thereby guaranteeing the integrity of representation learning. Moreover, removing the upper bound results in a significant increase in computational overhead. The upper bound prevents “hub nodes” from monopolizing experts, ensuring load balance and efficiency.

Impact of Orthogonality. It is worth noting that removing the prototype orthogonal loss (\mathcal{L}_o) results in the most drastic performance loss. This phenomenon profoundly reveals the core status of the orthogonality constraint: it forces experts to maintain differentiation in the feature space, preventing the problem of expert homogenization (Collapse). By maximizing the mutual exclusivity between experts, this mechanism ensures that the model can capture diverse and complementary semantic features in the data, rather than repeatedly learning similar patterns.

3.4. Parameter Sensitivity Analysis

To further validate the model’s sensitivity to hyperparameters, we conduct a detailed parameter sensitivity analysis on four core hyperparameters in HOPE using the Ogbn-mag dataset with backbone HGAMLP. Figure 2 illustrates the impact of parameter changes on model performance.

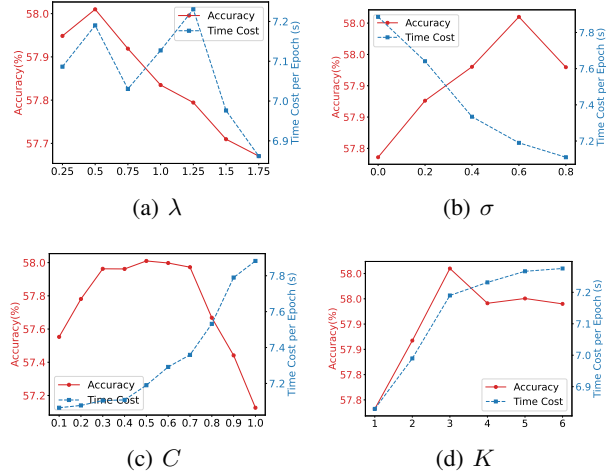


Figure 2. Hyper-parameter analysis.

Impact of Orthogonality Constraint Weight (λ). Experimental results show that as λ gradually increases from 0.25 to 0.5, model performance exhibits an upward trend, but when λ exceeds 0.5, performance begins to decline significantly. This “inverted U-shaped” trend reveals a trade-off between diversity and fitting capability. A moderate λ is crucial for preventing expert homogenization (Mode Collapse), as it forces experts to learn complementary semantic patterns. However, an excessively large penalty coefficient overly constrains the parameter space of the experts, limiting their flexibility to fit the true data distribution, leading to underfitting.

Impact of Similarity Threshold (δ): Model performance peaks within the interval $\delta \in [0.4, 0.8]$, proving that this range is the optimal sweet spot for distinguishing valid signals from noise. When the threshold is too low ($\delta < 0.4$), the model introduces a large number of low-relevance noise

connections, which not only dilutes valid features but also increases unnecessary computational burdens; conversely, when the threshold is set too high ($\delta > 0.8$), valid connections with potential semantic associations are erroneously filtered out, leading to model degradation. At this point, the routing mechanism relies overly on mandatory lower-bound allocation, losing its capacity for flexible selection.

Impact of Lower Bound Capacity (K): For each expert, the minimum number of assigned nodes is $K \times B/N_E$, where B is the batch size, and N_E represents the number of experts. We observe that optimal range of K is $[0.6, 0.7]$. This parameter is directly related to the representation quality of long-tail nodes. An overly small lower bound causes some nodes with weak features to fail to obtain sufficient expert resources, becoming “orphan nodes” lacking effective gradient updates. While an overly large lower bound is counterproductive, forcing experts to process nodes irrelevant to their semantics, introducing severe interference noise, thereby damaging the specialization of the experts.

Impact of Upper Bound Capacity (C): For each expert, the maximum number of assigned nodes is $K \times B/N_E$, where B is the batch size, and N_E represents the number of experts. As C increases from 2 to 4, model performance experiences a sharp rise. The performance improvement in the initial stage indicates that appropriately relaxing the upper limit of expert capacity effectively alleviates the congestion problem caused by “Hub Nodes” and fully releases the expressive power of experts. However, when the capacity exceeds 4.0 times the average load, the model reaches a saturation state. At this point, further increasing the capacity upper limit no longer brings performance gains but only increases computational overhead, validating the necessity of finding a balance point between efficiency and performance.

4. Related Work

4.1. Heterogeneous Graph Neural Networks

HGNNs are now the paradigm for multi-relational graph modeling. Early methods evolved from simple relation-aggregation (e.g., R-GCN (Schlichtkrull et al., 2018)) to attention-based architectures, such as the hierarchical attention in HAN (Wang et al., 2019) and the Transformer-driven dynamic modeling in HGT (Hu et al., 2020). Subsequent research refined structural awareness via relation-guided attention (Wu et al., 2021) and cross-relation interaction learning (Yu et al., 2023). To improve efficiency, approaches like Simple-HGN (Lv et al., 2021b) and NARS (Yu et al., 2020) simplified edge embeddings and decoupled neighbor dependencies. More recently, SeHGNN (Yang et al., 2023) and HGMLP (Liang et al., 2024b) achieved state-of-the-art scalability by separating feature propagation from transformation and incorporating node-adaptive weighting.

Other works have focused on capturing complex topologies, addressing long-range dependencies (Wang et al., 2025) and multi-scale hierarchies (Li et al., 2025).

Despite these advances, most methods rely on a fixed-capacity global linear decoder. This design overlooks non-linear decision boundaries and fails to handle long-tail distributions, leading to under-fitting on hub nodes and over-smoothing on tail nodes.

4.2. Mixture-of-Experts

MoE enables efficient model scaling through conditional computation (Shazeer et al., 2017). Following foundational sparse gating works like GShard (Lepikhin et al., 2021) and Switch Transformer (Fedus et al., 2022), research has shifted toward optimizing routing strategies for better load balancing (Zhou et al., 2022) and differentiability (Puigcerver et al., 2024). Additionally, integrating parameter-efficient tuning with experts (e.g., LoRAMoE (Dou et al., 2023), MoLE (Wu et al., 2024)) offers a viable path for resource-constrained training.

MoE in Graphs. Current applications of MoE in graphs primarily enhance the encoder’s ability to handle semantic and structural diversity. Methods like GME (Wang et al., 2023), MoGL (Zhou et al., 2025), and MoE-HGT (Mao & Sun, 2025) deploy experts to capture varied connectivity patterns and heterogeneous semantics. Innovations also extend to geometric spaces, with GraphMoRE (Guo et al., 2025) utilizing Riemannian experts, and structural learning, where approaches like MoSE (Ye et al., 2025) and DA-MoE (Yao et al., 2025) focus on motif encoding and adaptive receptive fields.

However, existing innovations are restricted to the encoding phase. The decoding stage typically defaults to a static, linear projection. This uniform decision boundary is ill-suited for the complex non-linear patterns and long-tail semantic disparities inherent in heterogeneous graphs.

5. Conclusion

To address the “Fixed Linear Projection Bottleneck” in HGNNs, we propose HOPE (Heterogeneous-aware Orthogonal Prototype Experts), a plug-and-play MoE framework. By integrating prototype-based routing, elastic capacity, and orthogonality constraints, HOPE effectively captures diverse and long-tail semantics. Experiments on four datasets confirm that HOPE consistently boosts SOTA performance in node classification and link prediction tasks with minimal overhead, validating the paradigm shift from static linear heads to dynamic expert decoding.

Impact Statement

This paper presents work whose goal is to advance the field of Machine Learning. There are many potential societal consequences of our work, none which we feel must be specifically highlighted here.

References

Cai, W., Jiang, J., Wang, F., Tang, J., Kim, S., and Huang, J. A survey on mixture of experts in large language models. *IEEE Transactions on Knowledge and Data Engineering*, 37(7):3896–3915, 2025.

Dong, Y., Chawla, N. V., and Swami, A. metapath2vec: Scalable representation learning for heterogeneous networks. In *Proceedings of the 23rd ACM SIGKDD international conference on knowledge discovery and data mining*, pp. 135–144, 2017.

Dou, S., Zhou, E., Liu, Y., Gao, S., Zhao, J., Shen, W., Zhou, Y., Xi, Z., Wang, X., Fan, X., et al. Loramoe: Revolutionizing mixture of experts for maintaining world knowledge in language model alignment. *arXiv preprint arXiv:2312.09979*, 2023.

Fedus, W., Zoph, B., and Shazeer, N. Switch transformers: Scaling to trillion parameter models with simple and efficient sparsity. *Journal of Machine Learning Research*, 23(120):1–39, 2022.

Guo, Z., Sun, Q., Yuan, H., Fu, X., Zhou, M., Gao, Y., and Li, J. Graphmore: Mitigating topological heterogeneity via mixture of riemannian experts. In *Proceedings of the AAAI Conference on Artificial Intelligence*, pp. 11754–11762, 2025.

Hu, Z., Dong, Y., Wang, K., and Sun, Y. Heterogeneous graph transformer. In *Proceedings of the Web Conference 2020*, pp. 2704–2710, 2020.

Lepikhin, D., Lee, H., Xu, Y., Chen, D., Firat, O., Huang, Y., Krikun, M., Shazeer, N., and Chen, Z. Gshard: Scaling giant models with conditional computation and automatic sharding. In *Proceedings of the International Conference on Learning Representations*, pp. 1–23, 2021.

Li, J., Sun, Z., He, X., Zeng, L., Lin, Y., Li, E., Zheng, B., Zhao, R., and Chen, X. Locmoe: a low-overhead moe for large language model training. In *Proceedings of the Thirty-Third International Joint Conference on Artificial Intelligence*, pp. 6377–6387, 2024.

Li, S., Gong, J., Ke, S., and Tang, S. Graph transformer-based heterogeneous graph neural networks enhanced by multiple meta-path adjacency matrices decomposition. *Neurocomputing*, 629:129604, 2025.

Liang, L., Xu, Z., Song, Z., King, I., Qi, Y., and Ye, J. Tackling long-tailed distribution issue in graph neural networks via normalization. *IEEE Transactions on Knowledge and Data Engineering*, 36(5):2213–2223, 2024a.

Liang, Y., Zhang, W., Sheng, Z., Yang, L., Jiang, J., Tong, Y., and Cui, B. Hgamp: Heterogeneous graph attention mlp with de-redundancy mechanism. In *Proceedings of the 2024 IEEE 40th International Conference on Data Engineering*, pp. 2779–2791, 2024b.

Liu, Z., Nguyen, T.-K., and Fang, Y. Tail-gnn: Tail-node graph neural networks. In *Proceedings of the 27th ACM SIGKDD conference on knowledge discovery & data mining*, pp. 1109–1119, 2021.

Lv, Q., Ding, M., Liu, Q., Chen, Y., Feng, W., He, S., Zhou, C., Jiang, J., Dong, Y., and Tang, J. Are we really making much progress? revisiting, benchmarking and refining heterogeneous graph neural networks. In *Proceedings of the 27th ACM SIGKDD conference on knowledge discovery and data mining*, pp. 1150–1160, 2021a.

Lv, Q., Ding, M., Liu, Q., Chen, Y., Feng, W., He, S., Zhou, C., Jiang, J., Dong, Y., and Tang, J. Are we really making much progress? revisiting, benchmarking and refining heterogeneous graph neural networks. In *Proceedings of the 27th ACM SIGKDD conference on knowledge discovery & data mining*, pp. 1150–1160, 2021b.

Mao, Q. and Sun, J. Mixture of experts enhanced heterogeneous graph transformer. In *Proceedings of the International Conference on Knowledge Science, Engineering and Management*, pp. 92–103, 2025.

Mu, S. and Lin, S. A comprehensive survey of mixture-of-experts: Algorithms, theory, and applications. *arXiv preprint arXiv:2503.07137*, 2025.

Puigcerver, J., Ruiz, C. R., Mustafa, B., and Houlsby, N. From sparse to soft mixtures of experts. In *Proceedings of the International Conference on Learning Representations*, pp. 1–11, 2024.

Qiu, Z., Huang, Z., Zheng, B., Wen, K., Wang, Z., Men, R., Titov, I., Liu, D., Zhou, J., and Lin, J. Demons in the detail: On implementing load balancing loss for training specialized mixture-of-expert models. *arXiv preprint arXiv:2501.11873*, 2025.

Schlichtkrull, M., Kipf, T. N., Bloem, P., Berg, R. v. d., Titov, I., and Welling, M. Modeling relational data with graph convolutional networks. In *Proceedings of the 15th International Conference on Extended Semantic Web Conference*, pp. 593–607, 2018.

Shazeer, N., Mirhoseini, A., Maziarz, K., Davis, A., Le, Q., Hinton, G., and Dean, J. Outrageously large neural networks: The sparsely-gated mixture-of-experts layer. In *Proceedings of the International Conference on Learning Representations*, pp. 1–19, 2017.

Tang, J., Qu, M., Wang, M., Zhang, M., Yan, J., and Mei, Q. Line: Large-scale information network embedding. In *Proceedings of the 24th international conference on world wide web*, pp. 1067–1077, 2015.

Trouillon, T., Welbl, J., Riedel, S., Gaussier, É., and Bouchard, G. Complex embeddings for simple link prediction. In *Proceedings of the International conference on machine learning*, pp. 2071–2080. PMLR, 2016.

Veličković, P., Cucurull, G., Casanova, A., Romero, A., Liò, P., and Bengio, Y. Graph Attention Networks. In *Proceedings of the International Conference on Learning Representations*, pp. 1–12, 2018.

Wang, H., Jiang, Z., You, Y., Han, Y., Liu, G., Srinivasa, J., Kompella, R. R., and Wang, Z. Graph mixture of experts: learning on large-scale graphs with explicit diversity modeling. In *Proceedings of the 37th International Conference on Neural Information Processing Systems*, pp. 50825–50837, 2023.

Wang, K., Shen, Z., Huang, C., Wu, C.-H., Dong, Y., and Kanakia, A. Microsoft academic graph: When experts are not enough. *Quantitative Science Studies*, 1(1):396–413, 2020.

Wang, S., Cao, G., Cao, W., and Li, Y. Nla-gnn: Non-local information aggregated graph neural network for heterogeneous graph embedding. *Pattern Recognition*, 158:110940, 2025.

Wang, X., Ji, H., Shi, C., Wang, B., Ye, Y., Cui, P., and Yu, P. S. Heterogeneous graph attention network. In *Proceedings of the The world wide web conference*, pp. 2022–2032, 2019.

Wu, X., Jiang, M., and Liu, G. R-gsn: The relation-based graph similar network for heterogeneous graph. *arXiv preprint arXiv:2103.07877*, 2021.

Wu, X., Huang, S., and Wei, F. Mixture of lora experts. In *Proceedings of the International Conference on Learning Representations*, pp. 1–17, 2024.

Yang, C., Xiao, Y., Zhang, Y., Sun, Y., and Han, J. Heterogeneous network representation learning: A unified framework with survey and benchmark. *IEEE Transactions on Knowledge and Data Engineering*, 34(10):4854–4873, 2022. doi: 10.1109/TKDE.2020.3045924.

Yang, X., Yan, M., Pan, S., Ye, X., and Fan, D. Simple and efficient heterogeneous graph neural network. In *Proceedings of the the AAAI Conference on Artificial Intelligence*, pp. 10816–10824, 2023.

Yao, Z., Chen, M., Liu, C., Meng, X., Zhan, Y., Wu, J., Pan, S., Xu, H., and Hu, W. Da-moe: addressing depth-sensitivity in graph-level analysis through mixture of experts. *Neural Networks*, pp. 108064, 2025.

Ye, J., Zhang, Z., Sun, L., and Luo, S. Mose: Unveiling structural patterns in graphs via mixture of subgraph experts. *arXiv preprint arXiv:2509.09337*, 2025.

Yu, L., Shen, J., Li, J., and Lerer, A. Scalable graph neural networks for heterogeneous graphs. *arXiv preprint arXiv:2011.09679*, 2020.

Yu, L., Sun, L., Du, B., Liu, C., Lv, W., and Xiong, H. Heterogeneous graph representation learning with relation awareness. *IEEE Transactions on Knowledge and Data Engineering*, 35(6):5935–5947, June 2023.

Zeng, Y., Huang, C., Mei, Y., Zhang, L., Su, T., Ye, W., Shi, W., and Wang, S. Efficientmoe: Optimizing mixture-of-experts model training with adaptive load balance. *IEEE Transactions on Parallel and Distributed Systems*, 36(4):677–688, 2025.

Zhou, G., Xu, Z., Yang, K., Wang, J., Lu, Z., and Li, T. Mogl: A mixture of heterogeneous experts for collaborative graph learning. *Neural Networks*, pp. 108503, 2025.

Zhou, W., Huang, H., Shi, R., Song, X., Lin, X., Wang, X., and Jin, H. Temporal heterogeneous information network embedding via semantic evolution. *IEEE Transactions on Knowledge and Data Engineering*, 35(12):13031–13042, 2023.

Zhou, W., Huang, H., Shi, R., Yin, K., and Jin, H. An efficient subgraph-inferring framework for large-scale heterogeneous graphs. In *Proceedings of the AAAI Conference on Artificial Intelligence*, pp. 9431–9439, 2024.

Zhou, Y., Lei, T., Liu, H., Du, N., Huang, Y., Zhao, V. Y., Dai, A., Chen, Z., Le, Q., and Laudon, J. Mixture-of-experts with expert choice routing. In *Proceedings of the 36th International Conference on Neural Information Processing Systems*, pp. 7103–7114, 2022.

Table 4. Link prediction results. OOM denotes Out of Memory, and table shows the time spent in one epoch.

	Yelp					DBLP				
	#Parma	Training	Inferring	AUC	Precision	#Parma	Training	Inferring	AUC	Precision
R-GCN	0.11M	64.90s	435.38s	28.57 \pm 0.17	43.13 \pm 0.12				OOM	
with HOPE	0.14M	63.88s	437.69s	30.74 \pm 0.15	46.52 \pm 0.18				OOM	
R-GAT	0.11M	64.78s	425.73s	36.46 \pm 8.62	44.33 \pm 4.41				OOM	
with HOPE	0.14M	67.14s	448.56s	39.02 \pm 6.11	46.75 \pm 3.26				OOM	
R-GSN		OOM					OOM			
with HOPE		OOM					OOM			
NARS	3.8M	9.56s	15.22s	75.52 \pm 2.91	76.08 \pm 2.47				OOM	
with HOPE	4.0M	10.24s	18.33s	76.90 \pm 2.64	78.86 \pm 2.44				OOM	
SeHGNN	6.22M	4.86s	5.38s	74.69 \pm 1.83	67.26 \pm 1.57	3.03M	8.49s	7.85s	53.09 \pm 0.26	51.79 \pm 0.15
with HOPE	8.44M	5.39s	5.42s	77.40 \pm 1.27	69.49 \pm 1.35	3.97M	9.04s	7.93s	56.11 \pm 0.32	54.58 \pm 0.19
HGAMLP	5.83M	4.23s	4.47s	77.86 \pm 0.66	72.75 \pm 1.38	2.93M	9.99s	8.19s	52.98 \pm 0.39	51.72 \pm 0.20
with HOPE	8.05M	4.89s	4.90s	79.69 \pm 0.57	75.57 \pm 1.06	3.87M	11.02s	8.98s	54.62 \pm 0.28	54.95 \pm 0.31

A. Link Prediction

To further validate the capabilities of HOPE, in addition to node classification, we evaluate its performance on the link prediction task using the Yelp and DBLP datasets. We employ Precision and AUC as evaluation metrics. The experimental results are summarized in Table 4. Similar to the node classification task, HOPE demonstrates strong performance enhancement capabilities in link prediction. After integrating HOPE into HGAMLP, Precision improves by 2.56% and AUC by 3.12%. Link prediction typically requires capturing finer-grained semantic relationships than node classification. Baseline models mainly rely on linear projections to aggregate neighborhood information, which often encounters bottlenecks when dealing with complex edge relationships. By introducing multiple orthogonal prototype experts, HOPE decouples features originally compressed in a single linear space into multiple complementary semantic subspaces. The significant improvement in experimental data demonstrates that HOPE successfully enriches node representations, enabling more accurate prediction of potential connections. Link prediction tasks often involve a large number of low-degree long-tail nodes. HOPE’s elastic capacity allocation mechanism plays a key role here. By setting a lower bound K , it ensures that even sparsely connected nodes are allocated sufficient expert computational resources, avoiding the “representation collapse” problem common in traditional Top-K routing, thereby improving the overall robustness of predictions.